RSC Advances

PAPER

View Article Online
View Journal | View Issue

Cite this: *RSC Adv.*, 2019, **9**, 23957

A thermoresponsive microfluidic system integrating a shape memory polymer-modified textile and a paper-based colorimetric sensor for the detection of glucose in human sweat†

Jing He,[ab] Gang Xiao,[ab] Xiaodie Chen,[ab] Yan Qiao,[ab] Dan Xu*[c] and Zhisong Lu*[ab]

Textile-based microfluidic analytical devices have demonstrated significant potentials in biomolecular detection; however, to date, they have not been integrated with a shape memory polymer to prepare a thermoresponsive device for human sweat analysis. Herein, a thermoresponsive textile/paper-based microfluidic analysis system was constructed by combining biocompatible polyurethane (PU), cotton fabric and a paper-based colorimetric sensor. The coating of PU endowed the textile with temperature-dependent shape memory capability and patterned the channels to guide the liquid transport. A paper-based colorimetric sensor was prepared *via* a layer-by-layer deposition method and coupled with a smartphone for the quantitative analysis of glucose concentration. The as-prepared thermoresponsive textile/paper-based microfluidic analysis system had the dynamic range of 50–600 μM and the detection limit of 13.49 μM. After being fixed in the inner collar of a shirt, the system demonstrated great capabilities for the thermal-triggered sweat transport and *in situ* detection of glucose in human sweat under a high-temperature condition (59 °C). This study not only provides a low-cost and easy-to-wear sweat analysis tool for the health monitoring of people working at high temperatures, but also expands the applications of shape memory polymers and textile-based microfluidic devices in point-of-care testing.

Received 15th April 2019
Accepted 18th July 2019

DOI: 10.1039/c9ra02831e

rsc.li/rsc-advances

1. Introduction

As an emerging field involving electronics, materials chemistry and biological science, wearable devices have attracted significant interest of academia and industry due to their great potential in daily health monitoring,[1] motion tracking,[2] and disease diagnostics.[3] A flexible sensor is the core component of a wearable device, which possesses excellent flexibility and the capability of converting biological events into measurable signals. In the past few years, flexible strain/stress sensors were the most extensively investigated wearable components.[4,5] They have been fabricated on various ultra-flexible substrates and perfectly conform to the human body to sense the slight changes in human skin.[6] The development of these sensors has significantly promoted the application of wearable systems in the real-time monitoring of basic vital signs such as pulse rate,[7] blood pressure[8] and respiration rate.[9]

Since the analysis of biomarkers at the molecular level plays an important role in precise clinical diagnosis and the surveillance of chronic diseases, significant efforts have been dedicated towards the development of wearable sensors for the *in situ* molecular analysis of bio-fluids.[10] Sweat is a typical body fluid containing plenty of chemical substances, such as ions, small molecules, proteins and hormones, closely correlated to the human physiological states.[11] Sweat has been deemed as the most promising candidate to replace conventional blood samples due to its easy and non-invasive harvesting from human body.[12] Wearable sensors can directly contact human skin at the sites of sweat production, allowing the rapid collection and detection of analytes before their degradation. Therefore, a wearable device would be an ideal system for human sweat analysis.

In recent years, various flexible and biocompatible materials have been employed as substrates to fabricate wearable sweat sensors.[13] Tattoo-based flexible sensors have been prepared *via* a screen-printing technique, enabling the transfer of electrodes on human skin for the reliable *in situ* measurement of lactate,

[a]*Key Laboratory of Luminescent and Real-Time Analytical Chemistry (Southwest University), Ministry of Education, School of Materials & Energy, Southwest University, 1 Tiansheng Road, Chongqing 400715, P. R. China. E-mail: zslu@swu.edu.cn; Fax: +86-23-68254969; Tel: +86-23-68254732*

[b]*Institute for Clean Energy & Advanced Materials, School of Materials & Energy, Southwest University, 1 Tiansheng Road, Chongqing 400715, P. R. China*

[c]*Department of Gastroenterology, The Central Hospital of Wuhan, Tongji Medical College, Huazhong University of Science and Technology, Shengli Street Jiang'an District No. 26, Wuhan 430014, P. R. China. E-mail: drxu0624@gmail.com*

† Electronic supplementary information (ESI) available. See DOI: 10.1039/c9ra02831e

pH and alcohol in sweat.[14] Gao *et al.* integrated a PET-based electrode array with a printed circuit board in the form of a wristband or headband for the *in situ* monitoring of multiple sweat analytes.[15] In addition to electrochemical sensors, a polydimethylsiloxane (PDMS)-based colorimetric microfluidic sensing system has been developed to detect chloride, glucose, and lactate in sweat. The network channels could spontaneously route sweat to the sensing area; this resulted in color change of chromogenic reagents.[16] Very recently, a textile-based colorimetric sensor has been manufactured *via* layer-by-layer deposition of chitosan, sodium carboxymethyl cellulose and an indicator dye or lactate assay reagents for the detection of sweat pH and lactate.[17] During its application, the modified textile was directly patched on human skin to adsorb the sweat secreted by the human body, triggering a colorimetric reaction. As a clothing material with thousands of years of history, textile has excellent flexibility, superior biocompatibility and tailorable hydrophilicity, which render it a promising substrate for the preparation of wearable sweat sensors. Although textile-based colorimetric sensors have already been reported for sweat analysis, the structure of the system still needs a rational design to avoid the possible contact of chemical reagents with human skin.

Microfluidic textile-based analytical devices have demonstrated significant potential to perform sophisticated processes for the detection of glucose,[18] hydrogen peroxide,[19] lactate[20] and proteins.[21] To date, the wax printing technique is still the most widely used approach for patterning hydrophobic and hydrophilic regions on textiles.[22] Shape-memory polymers (SMPs) are a group of polymeric materials that can return from the deformed state to their original state under external stimuli such as temperature change,[23] light irradiation,[24] and magnetic field alteration.[25] Among them, thermoresponsive SMP has been widely applied in the textile, aerospace, biomedicine and food packaging industries because of its easy synthesis and ultrahigh shape recovery rate.[26,27] In a relatively high temperature environment, human body can perspire heavily to produce sufficient sweat for non-invasive analysis. A high-temperature environment can affect the metabolic rates in the human body, further resulting in the alteration of blood glucose. High temperatures can also be utilized to trigger shape deformation of the specially designed SMP. Therefore, it is highly desirable to integrate SMP with a textile-based microfluidic analytical device for the development of a thermoresponsive textile-based microfluidic device capable of analyzing sweat secreted by workers in high-temperature workplaces such as steel factories and boiler rooms. The existence of a thermal-triggered transporting system can avoid the direct contact of the sensing unit with human skin. Thus, the device would only monitor glucose in the sweat in a high temperature environment.

Herein, polyurethane (PU), a biocompatible and thermal-sensitive polymer, was utilized to functionalize cotton fabric for the production of a thermoresponsive textile-based microfluidic device. The thermal-triggered shape recovery capability of the device was investigated in terms of the PU coating layers. The modification process was also characterized by scanning electron microscopy (SEM), Fourier transform infrared spectroscopy (FTIR) and contact angle assay. Since paper-based analytical devices have demonstrated great capability for the low cost, fast and sensitive detection of metal ions,[28–32] phenolic pollutants[33] and biological molecules,[34–38] the optimized thermoresponsive textile-based microfluidic component has been further integrated with a paper-based glucose colorimetric sensor. To quantitatively measure the glucose level in sweat, a smartphone-based software was used to convert the color of the paper sensor into RGB values. The feasibility of the system was also demonstrated by fixing the folded microfluidic device and the corresponding paper sensor on the lower and upper sides of the inner collar, respectively, to *in situ* analyze the sweat of the volunteer at relatively high temperatures.

2. Materials and methods

2.1. Materials and regents

Cotton fabric was obtained from Qinling Textile Co. Ltd (Xinjiang, China). Thermal-sensitive PU was a gift from Beijing Newwat Material Technology Co. Ltd (Beijing, China). GOD (>180 U mg^{-1}), HRP (200 U mg^{-1}), chitosan, TMB, glucose, NaCl and Na_2CO_3 were purchased from Aladdin Reagent Co. Ltd (Shanghai, China). Lactate (85 wt% in H_2O) and uric acid were bought from Sigma-Aldrich (Shanghai, China) and Adams-beta Co. Ltd (Shanghai, China), respectively. Waterproof spray (Nano protector) was obtained from TARRAGO, Spain. All other chemicals were of analytical grade and directly used in the present study without further purification. Deionized (DI) water was obtained by a Millipore water purification system with resistance less than 18 MΩ cm.

2.2. Preparation of artificial sweat

Artificial sweat was prepared according to the standard DIN ISO3696.[39] In brief, 5.0 g sodium chloride, 940 μL lactic acid and 1.0 g urea were successively dissolved in 1 L DI water. The solution pH was adjusted to ~6.0 with 0.1 M NaOH. Glucose powder was added to the solution under stirring to obtain artificial sweat containing different amounts of glucose.

2.3. Thermoresponsive property of the PU-coated cotton fabrics

Cotton fabrics were treated with a boiling Na_2CO_3 solution (10 g L^{-1}) under stirring for 5 min to remove the surface-binding wax. Then, the fabrics were rinsed with DI water until the pH changed to neutral. The as-prepared fabrics were cut into small square pieces with the size of 3 cm × 3 cm. PU was densely and uniformly brushed on both sides of the tape-protected fabrics and cured at 30 °C for 1 h to form a PU film on the cotton fabric. The cotton fabrics modified with different layers of PU were folded in half at the bending angle of 180°, followed by incubation at 30, 40, 50, 60 and 70 °C. The unfolding response of the PU-coated fabrics was evaluated in terms of the opening angle and the response time.

2.4. The PU-fabric-based microfluidic channel

The microfluidic channel was fabricated on a fabric, as shown in Scheme 1. The pre-engraved tapes were adhered on both sides of the fabric at the designated locations. PU was densely and uniformly brushed on both sides of the tape-protected fabrics and cured at 30 °C for 1 h to form a PU film on the cotton fabric. After removing the protecting adhesives, the PU-coated cotton fabric with a microfluidic channel was obtained. The fabric-based channels were fabricated with the widths of 4, 5, 6, 7 and 8 mm while maintaining the length of 3 cm. After treatment with plasma for 40 s, a sufficient volume of red ink was dropped on one end of the channel. The time for the ink to flow through the channel was determined to calculate the flow velocity.

2.5. Characterization of the fabrics with/without PU coating

The morphologies of the cotton fabrics with/without the PU coating were investigated using SEM (JSM-6510LV, JEOL, Tokyo, Japan). The surface chemical groups in the pure PU film and cotton fabrics with/without the PU coating were analyzed using an FTIR spectrometer (Nicolet 6700 FTIR, Thermo Electronic Corporation, USA). The hydrophilicity of the samples was characterized by measuring the contact angle (Shanghai Zhongchen Digital Technic Apparatus Co. Ltd, China). A drop of DI water was deposited on the sample, and the angle formed by the water drop in contact with the substrate surface was determined immediately.

2.6. Paper-based colorimetric glucose sensor

Filter papers (Whatman® Grade 3) were cut into small disks with the diameter of 1 cm. Moreover, eight microliters of 1 mg mL^{-1} chitosan solution prepared in 0.25% (v/v) acetic acid was dropped onto the paper disks and dried in a fume hood for ~3 min. GOD, HRP and TMB were dissolved in 0.01 M PBS buffer (pH 7.0) at the concentrations of 180 U mL^{-1}, 0.15 mg mL^{-1} and 15.0 mM, respectively. Then, the as-prepared HRP, GOD and TMB solutions were successively deposited on the chitosan-modified paper substrates. The functionalized paper disks were stored at 4 °C and used in the following experiments.

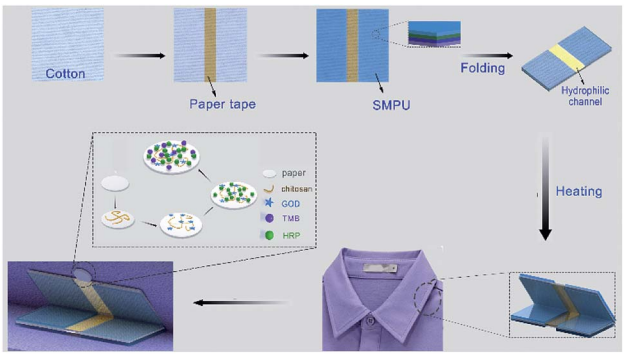

Scheme 1 Fabrication of the thermoresponsive textile/paper-based microfluidic sensing system.

2.7. Thermoresponsive microfluidic system

A cardboard was folded at the angle of 45°. A folded PU-fabric-based microfluidic channel and a paper-based sensor were attached to the upper and lower sides of the inner surface of the angle to form a thermoresponsive microfluidic system for the colorimetric detection of glucose. Artificial sweat samples containing 0, 50, 100, 200, 400 and 600 μM glucose were dropped at the open end of the channel to investigate the sensing performance. The entire system was placed at 60 °C to trigger the spring-back of the PU-fabric-based unit. When the microfluidic device opened up at a certain angle, the channel came in contact with the functionalized paper disk, guiding the liquid to the sensor element. The enzyme-catalyzed cascade reactions resulted in the gradual color change of the filter paper. The color of the paper disk was converted into RGB values with the assistance of a smartphone-based software (Color Name). All measurements were conducted at least three times.

2.8. Feasibility of the thermoresponsive microfluidic system

Herein, three healthy female volunteers were selected and made to stay at 59 °C. The folded PU-fabric-based microfluidic unit and the paper-based sensor were attached to the upper and lower sides of the inner surface of the volunteers' collars. The glucose levels in the sweat secreted by the volunteers were *in situ* detected using the thermoresponsive microfluidic systems. As abovementioned, the smartphone-based analysis was conducted to calculate the glucose concentrations.

3. Results and discussion

To optimize the thermoresponsive property of the textile-based device, the shape recovery capabilities of the textiles coated with different numbers of PU layers were evaluated at temperatures ranging from 30 to 70 °C. Before conducting the shape recovery assay, the PU-coated textiles were folded in half at the bending angle of 180°. The recovery angle was measured to represent the shape memory capability of the devices. It can be observed from

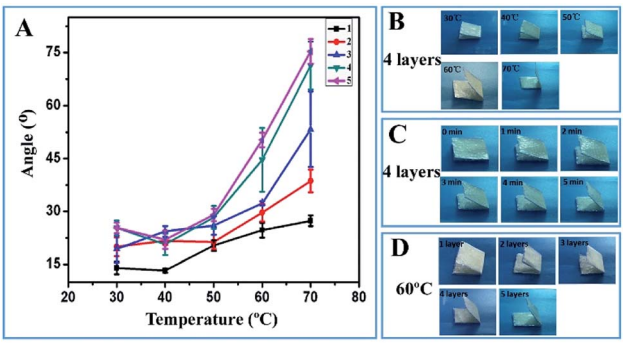

Fig. 1 (A) Recovery angle of the devices with different numbers of PU layers against the incubation temperature. (B) Images of the folded textiles with 4-layer PU after incubation at 30, 40, 50, 60 and 70 °C for 6 min; (C) images of the folded textiles with 4-layer PU after incubation at 60 °C for 0, 1, 2, 3, 4 and 5 min; and (D) images of the folded textiles with 1, 2, 3, 4 and 5 layers of PU after incubation at 60 °C for 6 min.

Fig. 1A that all devices gradually unfold at different temperatures. As the incubation temperature was increased from 30 to 70 °C, the maximum recovery angle of the PU-coated textile also increased (Fig. 1A and B). The recovery angle reached its maximum after 5 min; this indicated that the PU-modified textiles could respond very rapidly to relatively high temperatures (Fig. 1C). At temperatures lower than 50 °C, the influence of the PU layer thickness on the shape recovery property was not quite obvious. However, when the temperature was increased to 60 or 70 °C, the maximum recovery angle increased in a PU thickness-dependent manner (Fig. 1A and D). The data clearly showed that the PU coating layer endowed the textile with excellent thermoresponsive capability in the temperature range of 50–70 °C; thus, this textile could be adopted to fabricate a thermoresponsive microfluidic device in the following experiments; since there was no statistically significant difference in the temperature-triggered deformation between the textiles functionalized with 4-layers and those functionalized with 5-layers of PU, it was more efficient and cost-effective to fabricate 4-layer PU-coated textiles in the entire sensing system for the achievement of the thermoresponsive property.

SEM was conducted to investigate the surface morphology of the textile before and after the PU modification. The pristine cotton textile showed a typical woven structure with yarns tightly cross-linked with each other (Fig. 2A). After PU coating, a layer of the smooth film could be observed on the top of the woven structure, suggesting the successful deposition of PU on the cotton textile (Fig. 2B). From the side-view SEM image, the thickness of the 4-layer PU film could be measured as ~156 μm (Fig. 2C). FTIR spectroscopy was further carried out to characterize the surface chemical groups on the pristine and PU-coated textiles. The spectrum of the pristine cotton textile showed several characteristic peaks of cellulose macromolecules, which were located at 3325 cm^{-1} (O–H stretching), 2886 cm^{-1} (C–H stretching), 1424 cm^{-1} (C–H wagging), and 1029 cm^{-1} (C–O stretching), suggesting the effective removal of wax from the cotton textile. After the immobilization of PU, a strong peak at 1722 cm^{-1} and a weak peak at 1234 cm^{-1} appeared, which could be assigned to the –C=O stretching vibration and the C–O symmetric shrinkage vibration, respectively. Moreover, two more peaks caused by the –NH vibration could be found at 2946 and 1545 cm^{-1}. In addition, the coating of PU shielded the characteristic IR absorption peaks of cotton. The results strongly proved that the shape-memory polymer had fully covered the textile surface, agreeing well with the SEM data.

During the PU coating process, a textile band was protected to serve as the sweat transport channel without external pumps in the designed sensing system. Thus, it was necessary to characterize the liquid wicking property of the cotton textile-based microfluidic channel. A drop of water was completely absorbed into the textile in only 0.026 s (Fig. 3A); this showed the excellent water absorption capability of the textile. The width of the textile channel was further optimized by measuring the flow velocity of an ink solution. As shown in Fig. 3B–D, the ink solution could be transported along the textile channels. When the width was varied from 4 to 8 mm, the average flow velocity gradually reduced from 0.32 cm s^{-1} to 0.13 cm s^{-1}. Undoubtedly, more liquid was needed to fill up the device with wider channels. In practical applications, the perspiration rate may not meet the absorption rate of the textile channel. Therefore, to quicken the sweat transport and assay process, we needed to keep the channel as narrow as possible. Considering the test duration, the liquid transport efficiency and the difficulty of device fabrication, 4 mm was chosen as the optimal channel width for the preparation of PU-textile-based microfluidic devices.

Glucose is a very important small molecule present in sweat, which can be used to estimate the physiological status of the human body in a high-temperature environment.[40–43] In the present study, glucose was chosen as the target analyte to construct the sensing unit in the sweat analysis system. The filter paper-based colorimetric sensor was fabricated by successive modifications of paper disks with chitosan, GOD, HRP and TMB. The addition of chitosan provided a large number of amino groups for the high-density immobilization

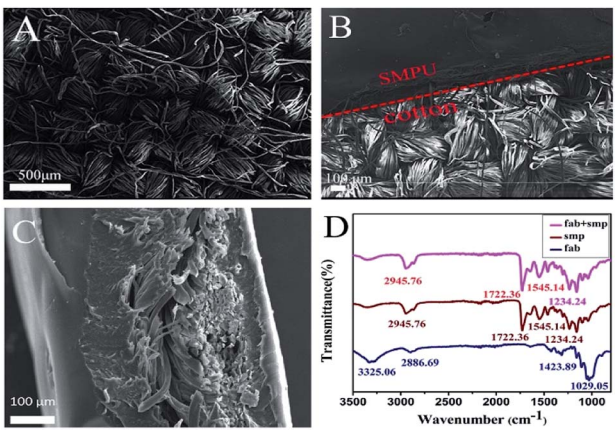

Fig. 2 (A) Surface morphology of the pristine cotton textile; (B) surface morphology of the border between the PU layer and the textile; (C) side-view of a PU-coated textile; and (D) FTIR spectra of the pristine textile, pure PU and PU-coated textile.

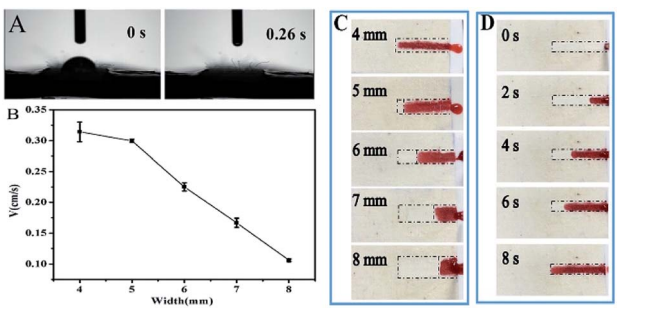

Fig. 3 (A) Liquid-wicking property of the textile channel; (B) correlation between the width of the textile channel and the average flow velocity; (C) images showing the transport of red ink in textile channels with the widths of 4, 5, 6, 7 and 8 mm after 8 s; and (D) images extracted from a video illustrating the transport of red ink in a textile channel with the width of 4 mm at 0, 2, 4, 6 and 8 s.

and even distribution of enzymes on the cellulose fibers, further leading to uniform coloring of the papers. As shown in Fig. S1 and S2 (ESI†), the amount of each reagent and the reaction time were optimized, respectively. During the assay, artificial sweat samples containing 0, 50, 100, 200, 400 and 600 μM glucose were directly dropped onto the sensors to initiate an enzyme-catalyzed reaction. It can be observed from Fig. 4A that the paper changes from white to blue. The higher the sweat glucose level, the darker the color of the paper. These results indicate that color alteration may be closely correlated to the glucose concentration in the sample. To further quantitatively determine the correlation between the sensor color and the glucose level, a smartphone-based platform was applied to obtain the sensor images and convert the colors into the *R*, *G* and *B* values. The color alteration induced by 200 μM glucose was compared in terms of the *R*, *G* and *B* values (Fig. 4B), showing that the *R* value had the most significant difference. Thus, the *R* value was utilized to evaluate the sensor performance and analyze glucose in the sweat in the following experiments. As illustrated in Fig. 4C, there was a negative linear correlation between the *R* value and the logarithm of glucose concentration in the range from 50 to 600 μM. The correlation could be expressed by the following equation:

$$V_R = 310.16 - 97.52 \lg C_{(glucose)} \ (R^2 = 0.99)$$

where V_R and $C_{(glucose)}$ represent the *R* value of the sensing paper and the glucose concentration, respectively. The limit of detection (LOD) of the sensor was calculated to be 10.4 μM (LOD $= 3\sigma/S$). It has been reported that the glucose concentration in human sweat varies in the range from 10 to 200 μM, which matches well with the dynamic range and LOD of the as-prepared sensor. Therefore, the paper-based colorimetric glucose sensor could be used as the sensing unit to be integrated with the PU-textile-based microfluidic device for the construction of a thermoresponsive glucose analyzing system.

A cardboard was folded at the angle of 45° to mimic the shirt collar in practical applications. The PU-textile-based device was folded in half and attached to one of the inner sides of the cardboard angle. The paper-based sensing unit was fixed at the other inner side of the angle, enabling the contact of the textile channel with the sensor after the thermal-triggered deformation of the microfluidic device (Fig. 5A and B). When the environmental temperature reached 60 °C, the microfluidic device gradually opened up and remained stable at the angle of 45° after 6 min (Fig. 5C). The opening end of the textile channel came in contact with the paper-based sensor, guiding the flow of the liquid sample to the sensing unit for the colorimetric detection of glucose (Fig. 5D). To verify the performance of the thermoresponsive sensing system, artificial sweat containing glucose at different concentrations was transported to the paper-based sensing unit *via* the textile channel. The results obtained were consistent with the findings shown in Fig. 4 that the reaction of glucose with the sensor induced the change of paper color from white to blue, and the color became darker in a dose-dependent manner (Fig. 5E). The calibration curve was plotted with *R* value *versus* the logarithm of glucose concentration, showing a very good linear correlation ($V_R = 293.21 - 88.86 \lg C_{(glucose)}$, $R^2 = 0.99$) in the concentration range from 50 to 600 μM (Fig. 5F). The LOD of the sensing system was calculated as 13.49 μM. The sensing performance of the as-prepared device was comparable to that of previously reported sweat glucose sensors (Table S1 in the ESI†). Furthermore, the sensing system and the calibration curve were utilized to investigate the artificial sweat spiked with 80, 160 and 320 μM glucose. The recovery ratios ranged from 76.72 ± 1.79% to 108.87 ± 2.54% (Table 1), which verified the good accuracy and reliability of the sensing system in detecting glucose in sweat. The results obtained herein indicate that a high temperature (60 °C) can trigger the deformation of the PU-textile microfluidic device to transport the sweat sample to the paper-based sensing unit for the accurate and reliable measurement of glucose. The thermoresponsive shape recovery process did not affect the glucose colorimetric sensing performance. Thus, the integrated system could be potentially applied for the *in situ* analysis of sweat secreted by humans in a high-temperature environment.

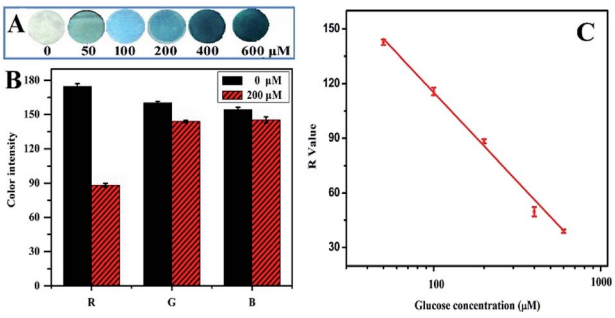

Fig. 4 (A) Images of the paper-based colorimetric sensors obtained after testing a series of artificial sweat samples containing 0, 50, 100, 200, 400 and 600 μM glucose; (B) the *R*, *G* and *B* values of the artificial sweat samples spiked with 0 and 200 μM glucose; and (C) plot of the *R* values against the logarithm of glucose concentrations. The experiments were conducted at 60 °C and repeated three times.

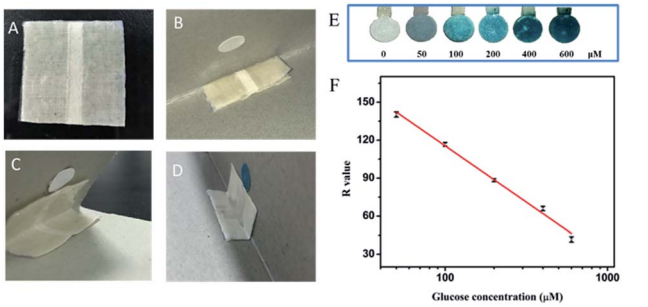

Fig. 5 (A) The PU-textile-based microfluidic device; (B) attachments of the PU-textile-based microfluidic device and the paper-based sensor; (C) operation of the system at 60 °C; (D) detection of glucose in artificial sweat using the system; (E) analysis of artificial sweat samples containing 0, 50, 100, 200, 400, 600 μM glucose by the thermoresponsive textile/paper-based microfluidic sensing systems; and (F) calibration curve for the thermoresponsive textile/paper-based microfluidic sensing systems. The experiments were conducted at 60 °C and repeated three times.

Table 1 Recovery ratio of glucose spiked in artificial sweat

Spiked $C_{Glucose}$ (μM)	Measured $C_{Glucose}$ (μM, mean ± SD, $n = 3$)	Recovery ratio (%) (mean ± SD, $n = 3$)
80	61.37 ± 2.07	76.72 ± 1.79%
160	144.34 ± 2.21	90.22 ± 2.16%
320	348.37 ± 2.46	108.87 ± 2.54%

To verify the feasibility of the thermoresponsive textile/paper-based microfluidic sensing system for sweat analysis, the system was incorporated under the collar of a shirt for the *in situ* detection of human sweat glucose in a high-temperature environment. During the on-body assay, three healthy female volunteers wearing the functionalized shirt stayed in a room at the temperature of 59 °C. After 15 min, the PU-textile-based device opened up, and the volunteers began to sweat heavily. The sweat flowed along the textile channel to the sensing unit and infiltrated it completely, initiating the multi-enzyme cascaded reactions for the *in situ* glucose detection. To investigate the effect of the amount of sweat on the detection of glucose, different volumes of sweat (6, 14 and 22 μL) were added to the devices, as shown in Fig. S3.† It could be observed that an incomplete infiltration of the sensing unit could influence the measurement. However, in the completely infiltrated sensing papers, the additional volume of sweat could not significantly alter the quantitative analysis. In our on-body tests, the paper-based sensors were completely infiltrated by the sweat secreted by the volunteers. Thus, the glucose concentration could be quantitatively analyzed using a smartphone. It was found that the glucose concentrations in the sweat samples obtained from the three volunteers were 34.71 ± 2.93, 74.22 ± 1.95 and 224.24 ± 1.77 μM, which were in the healthy concentration range of sweat glucose. Since the glucose level in sweat is two orders of magnitude lower than that in blood, commercially available test strips and glucometers cannot be applied to analyze sweat samples. The thermoresponsive textile/paper-based microfluidic sensing system demonstrates great potential in the analysis of sweat secreted from people working in high-temperature environments. After careful calculation, we have estimated that each assay may cost only 0.37 USD (Fig. 6).

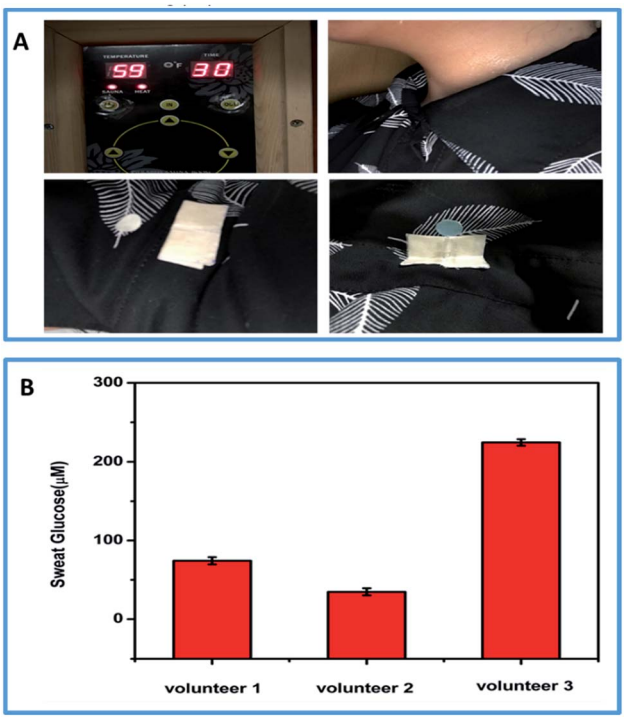

Fig. 6 (A) Practical application of the thermoresponsive textile/paper-based microfluidic sensing system for glucose detection in sweat secreted by volunteers in a high-temperature environment; (B) glucose concentrations in the sweat secreted by 3 female volunteers. The experiments were conducted at 59 °C and repeated three times.

4. Conclusions

In summary, we demonstrated a thermoresponsive microfluidic system integrating a shape-memory polymer-modified textile and a paper-based colorimetric sensor for the detection of glucose in human sweat. The shape memory PU was successfully coated on the textile to endow it with an excellent thermoresponsive property and prepare a microfluidic channel. At ~60 °C, the folded PU-textile-based microfluidic device could gradually open to guide the sweat to the paper-based glucose sensor, triggering enzyme-catalyzed colorimetric reactions. By coupling the system with a smartphone-based analysis platform, the glucose concentration could be quantitatively evaluated in terms of the R values. The thermoresponsive glucose sensing system showed the linear range of 50–600 μM and the detection limit of 13.49 μM. After being incorporated into the collar of a shirt, the system was adopted for the *in situ* detection of sweat glucose levels of three healthy volunteers in a high-temperature environment (~59 °C). Their sweat glucose concentrations were 34.71 ± 2.93, 74.22 ± 1.95 and 224.24 ± 1.77 μM. This study not only may provide a low-cost and easy-to-wear sweat monitoring tool for workers exposed to high temperatures, but may also expand the applications of shape memory polymers and textile-based microfluidic devices in human sweat analysis.

Conflicts of interest

There are no conflicts to declare.

Acknowledgements

This work was financially supported by the Fundamental Research Funds for the Central Universities (XDJK2019B002), Funding for Health Bureau of Wuhan (2014WX14A04) and Chongqing Engineering Research Center for Micro-Nano Biomedical Materials and Devices.

References

1 L. Yu, Y. Yi, T. Yao, Y. Z. Song, Y. R. Chen, Q. C. Li, Z. Xia, N. Wei, Z. N. Tian, B. Q. Nie, L. Zhang, Z. F. Liu and J. Y. Sun, *Nano Res.*, 2019, **12**, 331.

2 S. Bahadori, T. Immins and T. W. Wainwright, *J. Rehabil. Assist. Technol. Eng.*, 2018, **4**, 1.
3 S. Q. Wang, T. Chinnasamy, M. A. Lifson, F. Inci and U. Demirci, *Trends Biotechnol.*, 2016, **34**, 909.
4 J. Hwang, J. Jang, K. Hong, K. N. Kim, J. H. Han, K. Shin and C. E. Park, *Carbon*, 2011, **49**, 106.
5 Y. Pang, H. Tian, L. Q. Tao, Y. X. Li, X. F. Wang, L. Q. Deng, Y. Yang and T. L. Ren, *ACS Appl. Mater. Interfaces*, 2016, **8**, 26458.
6 M. Amjadi, K. Kyung, I. Park and M. Sitti, *Adv. Funct. Mater.*, 2016, **26**, 1678.
7 P. V. Boesen and V. Milevski, *US. Pat.* Application No. 15/443,244, 2017.
8 Y. Zheng, C. C. Y. Poon, B. P. Yan and J. Y. W. Lau, *J. Med. Syst.*, 2016, **40**, 1.
9 V. Jeyhani, T. Vuorinen, M. Mäntysalo and A. Vehkaoja, *Health and Technology*, 2017, **7**, 21.
10 J. Kim, A. S. Campbell and J. Wang, *Talanta*, 2018, **177**, 163.
11 A. Mena-Bravo and M. D. L. De Castro, *J. Pharm. Biomed. Anal.*, 2014, **90**, 139.
12 S. Anastasova, B. Crewther, P. Bembnowicz, V. Curto, H. M. Dlp, B. Rosa and G. Z. Yang, *Biosens. Bioelectron.*, 2016, **93**, 139.
13 M. Bariya, H. Y. Y. Nyein and A. Javey, *Nat. Electron.*, 2018, **1**, 160.
14 A. J. Bandodkar, W. Jia and J. Wang, *Electroanalysis*, 2015, **27**, 562.
15 W. Gao, S. Emaminejad, H. Y. Y. Nyein, S. Challa, C. Kevin, A. Peck, M. F. Hossain, O. Hiroki, S. Hiroshi, K. Daisuke, D. H. Lien, A. B. George, W. D. Ronald and A. Javey, *Nature*, 2016, **529**, 509.
16 A. Koh, D. Kang, Y. Xue, R. M. Pielak, J. Kim, T. Hwang, S. Min, A. Banks, P. Bastien, M. C. Manco, L. Wang, K. R. Ammann, K. I. Jang, P. Won, S. Han, R. Ghaffari, U. Paik, M. J. Slepian, G. Balooch, Y. Huang and J. A. Rogers, *Sci. Transl. Med.*, 2016, **8**, 1.
17 N. Promphet, P. Rattanawaleedirojn, K. Siralertmukul, N. Soatthiyanon, P. Potiyaraj, C. Thanawattano, J. P. Hinestroza and N. Rodthongkum, *Talanta*, 2019, **192**, 424.
18 J. Choi, D. Kang, S. Han, S. B. Kim and J. A. Rogers, *Adv. Healthcare Mater.*, 2017, **6**, 1601355.
19 A. Nilghaz, S. Bagherbaigi, C. L. Lam, S. M. Mousavi, E. P. Córcoles and D. H. B. Wicaksono, *Microfluid. Nanofluid.*, 2015, **19**, 317.
20 G. Baysal, F. Neşe Kök, L. Trabzon, H. Kizil, I. Gocek and B. K. Kayaoğlu, *Applied Mechanics and Materials*, Trans Tech Publications, 2014, vol. 490, p. 274.
21 M. Sekar, M. Pandiaraj, S. Bhansali, N. Ponpandian and C. Viswanathan, *Sci. Rep.*, 2019, **9**, 1.
22 W. Dungchai, O. Chailapakul and C. S. Henry, *Analyst*, 2010, **136**, 77.
23 T. Raidt, M. Schmidt, J. C. Tiller and F. Katzenberg, *Macromol. Rapid Commun.*, 2018, **39**, 1700768.
24 W. Wang, D. Shen, X. Li, Y. Yao, J. Lin, A. Wang, J. Yu, Z. L. Wang, S. W. Hong, Z. Lin and S. Lin, *Angew. Chem.*, 2018, **130**, 2161.
25 J. Huang, L. Cao, D. Yuan and Y. K. Chen, *ACS Appl. Mater. Interfaces*, 2018, **10**, 40996.
26 M. D. Hager, S. Bode, C. Weber and U. S. Schubert, *Prog. Polym. Sci.*, 2015, **49**, 3.
27 F. Pilate, A. Toncheva, P. Dubois and J. M. Raquez, *Eur. Polym. J.*, 2016, **80**, 268.
28 G. Sriram, M. P. Bhat, P. Patil, U. T. Uthappa, H. Y. Jung, T. Altalhi, T. Kumeria, T. M. Aminabhavi, R. K. Pai, Madhuprasad and M. D. Kurkuria, *TrAC, Trends Anal. Chem.*, 2017, **93**, 212.
29 H. Sun, Y. Jia, H. Dong, L. X. Fan and J. P. Zheng, *Anal. Chim. Acta*, 2018, **1044**, 110.
30 J. C. Hofstetter, J. B. Wydallis, G. Neymark, T. H. Reilly III, J. Harrington and C. S. Henry, *Analyst*, 2018, **143**(13), 3085.
31 X. Sun, B. Li, A. Qi, C. Tian, J. Han, Y. Shi, B. Lin and L. Chen, *Talanta*, 2018, **178**, 426.
32 J. Qi, B. Li, X. Wang, Z. Zhang, Z. Wang, J. Han and L. Chen, *Sens. Actuators, B*, 2017, **251**, 224.
33 J. Qi, B. Li, X. Wang, L. Fu, L. Luo and L. Chen, *Anal. Chem.*, 2018, **90**(20), 11827.
34 A. R. Bertão, N. Pires, A. M. Fonseca, O. S. G. P. Soares, M. F. R. Pereira, T. Dong and I. C. Neveset, *Sens. Actuators, B*, 2018, **261**, 66.
35 B. Li, Z. Zhang, J. Qi, N. Zhou, S. Qin, J. Choo and L. Chen, *ACS Sens.*, 2017, **2**(2), 243.
36 L. S. A. Busa, M. Maeki, A. Ishida, H. Tani and M. Tokeshi, *Sens. Actuators, B*, 2016, **236**, 433.
37 J. Ding, B. Li, L. Chen and W. Qin, *Angew. Chem., Int. Ed.*, 2016, **55**(42), 13033.
38 X. Wu, X. Wang, W. Lu, X. Wang, J. Li, H. You, H. Xiong and L. Chen, *J. Chromatogr. A*, 2016, **1435**, 30.
39 M. J. Hutchison and J. R. Scully, *Electrochim. Acta*, 2018, **283**, 806.
40 S. Nakata, T. Arie, S. Akita and K. Takei, *ACS Sens.*, 2017, **2**, 443.
41 R. Duffield, A. McCall, A. J. Coutts and J. J. Peiffer, *J. Sport. Sci.*, 2012, **30**, 957.
42 H. Lee, C. Song, Y. S. Hong, M. S. Kim, H. R. Cho, T. Kang, K. Shin, S. H. Choi, T. Hyeon and D. H. Kim, *Sci. Adv.*, 2017, **3**, e1601314.
43 M. M. Sugg, C. E. Konrad and C. M. Fuhrmann, *Int. J. Biometeorol.*, 2016, **60**, 663.